



Deposited via The University of Leeds.

White Rose Research Online URL for this paper:

<https://eprints.whiterose.ac.uk/id/eprint/189062/>

Version: Accepted Version

Article:

Yang, Z, Tate, JE, Rushton, CE et al. (2022) Detecting candidate high NO_x emitting light commercial vehicles using vehicle emission remote sensing. *Science of the Total Environment*, 823. 153699. ISSN: 0048-9697

<https://doi.org/10.1016/j.scitotenv.2022.153699>

© 2022 Elsevier B.V. All rights reserved. This manuscript version is made available under the CC-BY-NC-ND 4.0 license <http://creativecommons.org/licenses/by-nc-nd/4.0/>.

Reuse

This article is distributed under the terms of the Creative Commons Attribution-NonCommercial-NoDerivs (CC BY-NC-ND) licence. This licence only allows you to download this work and share it with others as long as you credit the authors, but you can't change the article in any way or use it commercially. More information and the full terms of the licence here: <https://creativecommons.org/licenses/>

Takedown

If you consider content in White Rose Research Online to be in breach of UK law, please notify us by emailing eprints@whiterose.ac.uk including the URL of the record and the reason for the withdrawal request.

1 **Detecting Candidate High NO_x Emitting Light Commercial** 2 **Vehicles Using Vehicle Emission Remote Sensing**

3 Zhuoqian Yang ^{1*}, James Tate ¹, Christopher Rushton ¹, Eleonora Morganti ¹,
4 Simon Shepherd ¹

5 ¹ Institute for Transport Studies, University of Leeds, Leeds, LS2 9JT, UK

6 * Corresponding Author Zhuoqian Yang, email: tszy@leeds.ac.uk

7 **Abstract:**

8 Vehicle emission remote sensing devices have been widely used for monitoring
9 and assessing the real-world emission performance of vehicles. They are also
10 well-suited to identify candidate high emitting vehicles as remote sensing surveys
11 measure the on-road, real-driving emissions (RDE) of a high proportion of the
12 operational vehicle fleet passing through a testing site. This study uses the
13 Gumbel distribution to characterise the fuel-specific NO_x emission rates
14 (grams.kg⁻¹) from diesel vans (formally referred to as light commercial vehicles or
15 LCVs) and screen candidate high emitting vehicles. Van emission trends of four
16 European countries (Belgium, Sweden, Switzerland and the UK) from Euro 3 to
17 Euro 6a/b have been studied, and the impact of road grade on candidate Euro
18 6a/b high-emitters is also evaluated. The measurements of Euro 6a/b fleets from
19 four countries are pooled together, and a consistent 4% of candidate high-
20 emitters are found in both class II and class III Euro 6a/b vans, accounting for an
21 estimated 24% and 21% total NO_x emissions respectively. The pooled four
22 country data is differentiated by vehicle models and manufacture groups. Engine
23 downsizing of Euro 6a/b class II vans is suspected to worsen the emission
24 performance when vehicles are driven under high engine load. The VW Group is
25 found to be the manufacture with cleanest NO_x emission performance in the Euro
26 6a/b fleets. By distinguishing high-emitters from normally behaving vehicles, a
27 more robust description of fleet behaviour can be provided and high-emitting
28 vehicles targeted for further testing by plume chasing or in an inspection garage.
29 If the vehicle is found to have a faulty, deteriorated or tampered emission after-
30 treatment system, the periodic vehicle inspection safety and environmental
31 performance certificate could be revoked.

32 **Keywords:** remote sensing, vans, NO_x emissions, high-emitters identification

33 1 Introduction

34 Road transport is a major contributor to nitrogen oxides (NO_x) concentrations,
35 which has negative effects on public health and the environment ([Pastorello and](#)
36 [Melios 2016](#)). Knowledge of the real-world vehicle emissions is important to
37 assess the effectiveness of current control measures and substantiate future
38 policy decisions. The discrepancy between real-world driving and type-approval
39 emissions for passenger cars has been made clear, where real-world emissions
40 can exceed emission limits several times for different Euro standards ([Weiss et](#)
41 [al. 2011](#); [Chen and Borken-Kleefeld 2014](#); [DfT 2016](#)). However, only a limited
42 amount of research ([ICCT 2019a](#); [Chen, Sun and Borken-Kleefeld 2020](#)) has
43 studied the real-world emission performance of vans, even though vans saw a
44 106.2% rise in traffic over the last 25 years (compared with 29.8% for cars and
45 12.8% for lorries) ([DfT 2020](#)), and was estimated to contribute 36.1% of NO_x
46 emissions from the road traffic sector in 2019 in the UK ([NAEI 2021](#)).

47 Researchers have been developing different methods to monitor the real-world
48 NO_x emissions from vehicles using laboratory (chassis dynamometer) tests
49 ([Demuyne et al. 2012](#); [Moody and Tate 2017](#)), on-board tests (portable
50 emissions measurement systems — PEMS) ([O'Driscoll et al. 2016](#); [Luján et al.](#)
51 [2018](#)), plume chasing ([Wang et al. 2011](#); [Lau et al. 2015](#)) and remote sensing
52 instruments ([Carslaw et al. 2011](#); [Chen and Borken-Kleefeld 2016](#)). Unlike
53 laboratory tests, PEMS or plume chasing that provide second by second emission
54 rates (grams.sec⁻¹) over a whole driving cycle or journey for a limited number of
55 test vehicles, remote sensing instruments un-intrusively takes a snap-shot
56 sample of fuel-specific emission rates (grams.kg⁻¹) from a large number of
57 vehicles in a single day ([Beaton et al. 1995](#); [Huang et al. 2018](#)). This makes
58 remote sensing a powerful approach for monitoring fleet emission characteristics
59 ([Carslaw et al. 2011](#); [Carslaw et al. 2013](#); [Chen and Borken-Kleefeld 2016](#);
60 [Grange et al. 2019](#)) and detecting candidate high-emitting vehicles ([Borken-](#)
61 [Kleefeld 2013](#); [Pujadas, Domínguez-Sáez and De la Fuente 2017](#); [Huang et al.](#)
62 [2019](#)).

63 When analysing remote sensing measurements some form of data aggregation
64 is needed as a single record is insufficient to derive meaningful, statistically
65 significant insights. The most common way to aggregate remote sensing data is
66 to calculate the mean emission rates classified by Euro standard and fuel type
67 ([Carslaw et al. 2011](#); [Chen and Borken-Kleefeld 2014](#)), based on an assumption
68 that the distribution of vehicle emissions is symmetrical, such as following a
69 normal distribution. However, previous remote sensing studies ([ICCT 2018](#);
70 [AWEL 2019](#); [Chen, Zhang and Borken-Kleefeld 2019](#)) have shown that vehicle

71 NO_x emissions are not normally distributed, rather skewed-right, making mean
72 emission statistics less appropriate to represent a group of remote sensing
73 measurements. Moreover, early studies often use arbitrary predetermined cut
74 points to identify high-emitters ([Pujadas, Domínguez-Sáez and De la Fuente
2017](#); [Huang et al. 2019](#)), regardless of the fact that the normal emission
75 performance may differ in a certain campaign site. Therefore further research is
76 considered to be needed to develop a more robust method to describe the fleet
77 behaviour and effectively distinguish high NO_x emitters from normally behaving
78 vehicles.
79

80 This paper uses the Gumbel distribution (explained in section 2.3) to analyse the
81 remote sensing measurements of diesel vans. Vehicles that follow the fitted
82 Gumbel distribution (referred to as 'on-model' vehicles) are selected to represent
83 the emission performance of the normally behaving vehicles in the operational
84 fleet, while the smaller and more highly emitting population which do not follow
85 the Gumbel distribution (referred to as 'off-model' vehicles) are regarded as
86 candidate high-emitters ([Rushton, Tate and Shepherd 2021](#)). Four European
87 countries' (Belgium, Sweden, Switzerland and the UK) remote sensing
88 campaigns during 2011-2019 have been selected from the CONOX project
89 ([Borken-Kleefeld et al. 2018a](#)) database and an overall fleet emission trend of
90 each country is studied. The impact of road grade on Euro 6a/b fleet in the Swiss
91 fleet is evaluated as this dataset includes a number of measurement sites with
92 relatively steep road gradients. Euro 6a/b fleet data from the four EU countries
93 are then combined based on two sample Kolmogorov-Smirnov test, and a more
94 differentiated degree of analysis by manufacture groups and models is conducted.

95 2 Materials and methods

96 2.1 The measurement principle

97 A vehicle emission remote sensing instrument is a monitoring system that has
98 been widely used to estimate the real-world vehicle emissions ([Beaton et al. 1995](#);
99 [Carslaw et al. 2011](#)). As shown in Figure 1-a, a remote sensing system positioned
100 at a roadside includes:

- 101 • A source & detector module which passes infrared and ultraviolet light
102 beams through the exhaust plume of passing vehicles and together with a
103 reflecting mirror measure the attenuation of light wavelengths. The
104 absorption of light is directly proportional to the concentration of pollutant
105 in the atmosphere, which includes the pollutant in the plume of the vehicle
106 crossed and in the background. After the background pollution is
107 subtracted, only the ratio of certain pollutant to CO₂ is reported ([Bishop
108 and Stedman 1996](#)), as the amount of plume seen is dependent on the
109 height of the tailpipe. Fuel-specific NO_x emission rates (in g/kg fuel burned)
110 can then be generated based on the fuel burnt in the engine ([Burgard et
111 al. 2006](#); [Carslaw et al. 2011](#)).
- 112 • A speed & acceleration detector which records the instantaneous speed
113 and acceleration of the vehicle passing by.
- 114 • A camera to capture the vehicle's number plate so that technical
115 characteristics (fuel type, Euro standard, make, model, etc.) of the vehicle
116 can be retrieved from national vehicle registration databases.

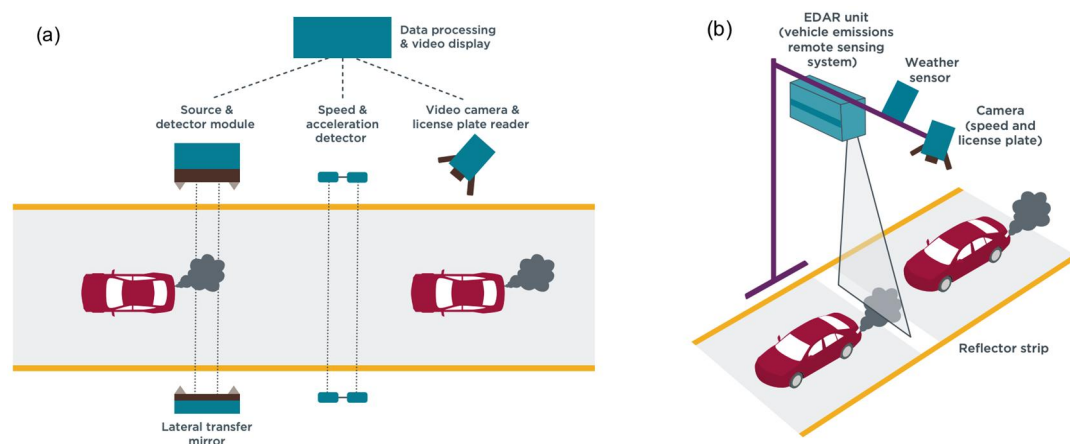


Figure 1 Schematics of a typical remote sensing deployment: (a) cross-road remote sensing system [left]; (b) top-down remote sensing system (EDAR) [right] ([Borken-Kleefeld and Dallmann 2018](#))

117 An alternative configuration is the EDAR instrument which emits a sheet of laser-
118 based infrared light in a top-down orientation, with a reflector strip mounted on
119 the road surface scattering back the laser light (see Figure 1-b). This deployment
120 means the measurements are less sensitive to the vehicle lane position, exhaust
121 position and wind speed ([Ropkins et al. 2017](#)).

122 **2.2 Data acquisition and preparation**

123 Remote sensing campaigns have been conducted in Europe since the early
124 1990's. In 2016, the Swiss Federal Office for the Environment (FOEN) founded
125 the CONOX (COmbining, COmparing and COllaborating on NO_x real driving
126 emission measurements) project, focusing on pooling, sharing, and analysing
127 European remote sensing data collected in a range of European cities over the
128 past 5 to 10 years ([Borken-Kleefeld et al. 2018b](#); [Sjödin et al. 2018](#); [Borken-
129 Kleefeld et al. 2018a](#)). The remote sensing data analysed in this paper are from
130 the CONOX project and include several remote sensing sampling campaigns
131 carried out during 2011-2019 across Belgium, Sweden, Switzerland and the UK.
132 As diesel vans account for 94% of van market in Europe ([ICCT 2019b](#)), this paper
133 only considers the emission performance of vans powered by diesel. A detailed
134 summary of fleet characteristics by country, Euro standard and class type¹ is
135 listed in Table A. 1 in the Appendix. The number of observations from Euro 3, 4,
136 5 and 6a/b diesel vans accessed and analysed is 106,662.

137 Remote sensing data also include measurements of the testing conditions
138 including ambient temperature, the road grade and the instantaneous speed and
139 acceleration of each passing vehicle. The test conditions differ between countries
140 as they are influenced by the characteristics of sample sites (road gradient,
141 vicinity of junctions etc), driver behaviour and prevailing meteorological
142 conditions. Based on the passing vehicles' speed/acceleration and campaign
143 site's road grade, equation and parameters provided by [Davison et al. \(2020\)](#), a
144 metric informing the instantaneous engine load called vehicle specific power
145 ([Jiménez-Palacios 1999](#)) is calculated. Vehicle Specific Power (VSP) value is a
146 useful metric when analysing remote sensing measurements as it characterises
147 the power demands on the engine and associated NO_x emissions ([Carslaw et al.
148 2013](#)). It can identify vehicles under high load (where high emissions are
149 expected) or at very low load (where fuel injection is disabled and plume sizes

¹ Van can be further classified into three sub-categories by reference mass, where class I are vans less than 1305kg, class II are those between 1305kg and 1760kg, and class III are those above 1760kg.

150 insufficient for valid remote sensing measurements) ([ICCT 2018](#)). As shown in
151 Table A. 1 in the Appendix, the average VSP value of each fleet is much higher
152 than the type approval NEDC² VSP value (around 4 kW/ton for vans). In other
153 words, most of the vehicles (Euro 3, 4, 5 and 6a/b) being measured have higher
154 engine load with either higher speed/acceleration or steeper road grade than the
155 test cycle. It is hypothesised that these vehicles have been designed to have
156 cleaner emission performance in NEDC-test-type conditions and less so for real-
157 world conditions ([Chen and Borken-Kleefeld 2014](#); [Triantafyllopoulos et al. 2019](#)).

158 Four remote sensing instruments, or generations of instrument, were used to
159 conduct the remote sensing campaigns being analysed, namely the RSD series
160 (RSD 4600 and RSD 5000) developed by Opus³, FEAT developed by University
161 of Denver⁴, and EDAR developed by HEAT⁵. The RSD series and FEAT are
162 cross-road remote sensing systems (shown in Figure 1-a) while EDAR is top-
163 down remote sensing system (shown in Figure 1-b). 35.0% Switzerland samples
164 and 22.8% UK samples were recorded by the RSD 4600 instrument which
165 doesn't have a NO₂ measurement capability, in which case estimated NO_x
166 (NO+NO₂) emission rates (grams.kg⁻¹) are generated from the measured NO and
167 an estimated contribution from NO₂. The measurement of primary NO₂ in the
168 exhaust has significant uncertainty and varies across remote sensing devices
169 ([Carslaw and Rhys-Tyler 2013](#); [Chen and Borken-Kleefeld 2014](#); [HBEFA 2019](#)).
170 However, in order to include samples measured by the RSD 4600 in this study,
171 a fixed ratio of NO₂: NO_x needs to be proposed. Among two of the devices (FEAT
172 and RSD 5000) that share the same measurement principle with RSD 4600, the
173 FEAT device is considered to have a more robust record of NO₂ emissions
174 compared with RSD 5000 ([Carslaw et al. 2019](#)), and it's measurement of NO has
175 been proven to have a strong correlation with the RSD 4600 ([Rushton et al. 2018](#)).
176 Therefore the fraction of primary NO₂ in NO_x (f_{NO2}) is directly derived from the
177 average ratio of NO₂ to NO_x emissions measured by FEAT in remote sensing
178 campaigns in the UK (detailed data for f_{NO2} by Euro standard and class type are
179 listed in Table A. 2 in the Appendix) and applied to RSD 4600 measurements.
180 Density plots of the fuel-specific NO_x emissions (grams.kg⁻¹) from both with and
181 without NO₂ measurement capability instruments are presented in Figure 2 (Euro
182 6a/b is not included because all Euro 6a/b samples were measured by devices
183 with NO₂ measurement capability). The different instruments are found to provide

² The New European Driving Cycle (NEDC) is a driving cycle used in European type-approval test. Average VSP value of NEDC cycle is also uniformly developed using the same equation and parameters, based on driving cycle's speed profile.

³ <https://www.opusrse.com/rsd-technology/>

⁴ <http://www.feat.biochem.du.edu/>

⁵ <https://www.heatremotesensing.com/edar>

184 comparable NO_x emissions within the same Euro standard and class type, which
 185 suggests it is appropriate to combine records measured by different instruments
 186 into a single dataset.

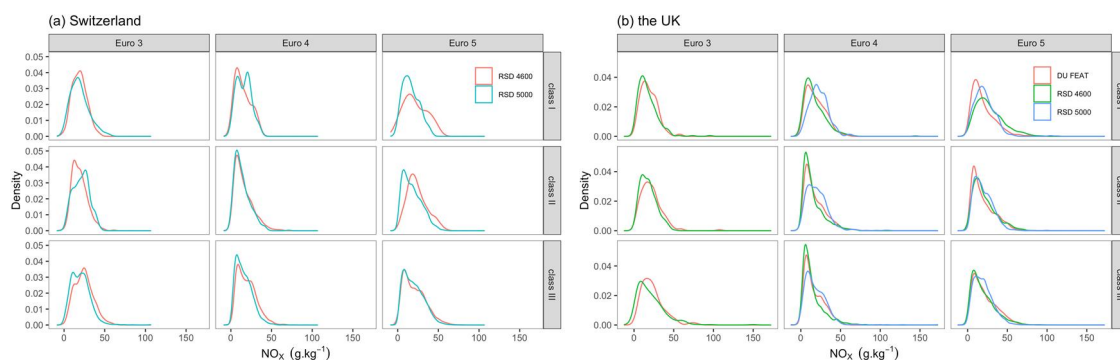


Figure 2 Density plot of NO_x emission rates (g/kg) for class I to class III vans by Euro standard and instrument in (a) Switzerland [left]; (b) the UK [right]

187 **2.3 The Gumbel distribution and maximum R^2 value method**

188 Figure 2 also demonstrates that the distribution of NO_x emissions measured in
 189 Switzerland and the UK has a skewed-right character and includes a proportion
 190 of extreme high emitting records. [Bishop et al. \(2016\)](#) and [Huang et al. \(2018\)](#)
 191 estimate that a small number of high-emitting vehicles could contribute a
 192 significant amount of total emissions, indicating that the emissions of the normally
 193 behaving vehicles would be elevated if simply using the mean emission statistics
 194 of a fleet. An accurate description of the remote sensing data distribution is
 195 essential in understanding the vehicle fleet behaviour. It does not only describe
 196 the average performance of the normally-behaving vehicles, but also identify
 197 candidate high-emitting vehicles.

198 The Gumbel distribution (Type-I Generalised Extreme Value distribution)
 199 ([Gumbel 1935](#)) is a right-skewed distribution function commonly used and widely
 200 adopted to model populations with a small number of extreme values that would
 201 not be captured by a normal distribution ([Sherif et al. 2014](#); [Ouarda et al. 2015](#);
 202 [Bhagat 2017](#); [Loucks and Beek 2017](#)). [Rushton, Tate and Shepherd \(2021\)](#)
 203 proposes using the Gumbel distribution to characterise passenger cars' remote
 204 sensing data. As diesel vans have similar emission characteristics to diesel
 205 passenger cars ([Chen, Sun and Borken-Kleefeld 2020](#)), the Gumbel distribution
 206 has also been applied to vans in this paper. The probability density function (*pdf*)
 207 $f(x)$ and cumulative density function (*cdf*) $F(x)$ of a Gumbel distribution are given
 208 as:

$$f(x) = \frac{1}{b} e^{-\left(\frac{x-a}{b} + e^{-\frac{x-a}{b}}\right)} \quad \text{Eq. 1}$$

$$F(x) = 1 - e^{-e^{-\frac{x-a}{b}}} \quad \text{Eq. 2}$$

209 Where a is the location parameter and represents the highest observation
210 frequency in a dataset; and b is the scale parameter and represents the spread
211 of the dataset.

212 When describing remote sensing measurements, the Gumbel distribution is
213 considered superior to other commonly used skewed-right distributions (Weibull,
214 Gamma, log-normal) as:

- 215 • The parameters in the Gumbel distribution are easy to interpret. The
216 location parameter a describes the emission rates that have been
217 recorded with the most frequency and scale parameter b determines the
218 statistical dispersion of the probability distribution; and
- 219 • The Gumbel distribution can be applied to negative values. In remote
220 sensing campaigns, small negative values are sometimes recorded
221 because of measurement noise and inaccurate determination of the
222 background concentration (e.g. a clean vehicle with very low emissions of
223 NO_x emissions follows with a short headway a high NO_x emitting vehicle)
224 ([Huang et al. 2018](#); [Smit et al. 2021](#)). These negative measurements
225 should be included and not rounded to zero ([Bishop, Burgard and
226 Stedman 2006](#); [McClintock 2011](#); [Gruening et al. 2019](#)), as this would
227 artificially uplift the negative values to zero and would inflate the average
228 values of the whole fleet.

229 It is hypothesised that the majority of the fleet follow the Gumbel distribution
230 except some extreme values, and these outliers are interpreted as candidate high
231 emitting vehicles ([Rushton, Tate and Shepherd 2021](#)). To test this hypothesis in
232 diesel vans, the distribution is cut successively by percentile, from 99% (vehicles
233 with the highest 1% NO_x emissions is removed from the whole fleet) to 1%
234 (vehicles in the top 99% NO_x emissions range is removed), and the Gumbel
235 distribution is re-applied to each sub-fleets. Then a goodness of fit test is used to
236 calculate R^2 value of observed and theoretical quantiles for each sub-fleet after
237 cutting. The sub-fleet with the maximum R^2 value is regarded as the 'on-model'
238 vehicle subset, and its corresponding Gumbel location parameter a is used to
239 represent the typical emission rate of the normally behaving vehicles in the whole
240 fleet, while scale parameter b determines the dispersion of the data. The
241 percentage of vehicles that do not follow Gumbel distribution are regarded as 'off-
242 model' percentage, and these vehicles are considered as candidate high emitting
243 vehicles. The detailed algorithm is given in Table 1.

Table 1 Algorithm for identifying the 'off-model' vehicles

Step 1: Apply the Gumbel distribution to the whole fleet F_{100}

Step 2: Calculate R^2 value of the observed and theoretical quantiles for fleet F_{100}

Step 3: Cut the fleet at each integer percentile starting from 99, apply the Gumbel distribution to $F_i, i = 99, 98, \dots, 1$

Step 4: Calculate R^2 value of observed and theoretical quantiles for fleet $F_i (F_{99}, F_{98}, \dots, F_1)$

Step 5: Repeat step 3-4 until there is no vehicle left in the fleet

Step 6: Create a dot plot of the cutting percentiles vs. the R^2 values

Step 7: Sub-fleet with the maximum R^2 value is regarded as the 'on-model' vehicle subset, and the fit parameters for the 'on-model' vehicles are the best description of the normally behaving vehicles in the whole fleet; the rest of the vehicles that do not follow Gumbel distribution are regarded as 'off-model' vehicles.

244 This method requires the original fleet to have a relatively large sample size,
245 because vehicles being regarded as 'off-model' vehicles usually only make up a
246 very small percentage of the whole fleet ([Rushton, Tate and Shepherd 2021](#)), if
247 the sample size is too small, no useful insight would be derived from the 'off-
248 model' vehicles. To ensure the statistical validity, the application of Gumbel
249 distribution to class I vans is not discussed in this paper as the Class I vans only
250 take account of 4.6% of the total measurements.

251 **2.4 A merged dataset**

252 Remote sensing data is often further segmented by VSP value ([Carslaw et al.](#)
253 [2013](#)), road grade ([Costagliola, Costabile and Prati 2018](#)), ambient temperature
254 ([Grange et al. 2019](#)) and make/model ([ICCT 2019a](#)) to study different factors'
255 impact on vehicle emissions. As each single country has only a relatively limited
256 number of samples, data from different countries needs to be combined together
257 to conduct analysis at a higher level of granularity. Here, the consistency of the
258 NO_x emission performance across fleets is checked before pooling data from
259 different countries. The two-sample Kolmogorov-Smirnov test (K-S test) is
260 applied to investigate whether the NO_x emission data from the four countries
261 share a statistically similar distribution. The two-sample K-S test is a
262 nonparametric hypothesis test that compares empirical distributions of two
263 samples and evaluates the largest absolute difference between the two
264 cumulative density functions ([Massey Jr 1951](#)) ([Lopes, Reid and Hobson](#)
265 [2007](#)). The test statistic D^* is given as:

$$D^* = \max(|\hat{F}_1(x) - \hat{F}_2(x)|) \quad \text{Eq. 3}$$

266 Where $\hat{F}_1(x)$ is the empirical cumulative density function of NO_x of sample 1, and
 267 $\hat{F}_2(x)$ is the empirical cumulative density function of NO_x of sample 2.

268 For sufficiently large sample size, the critical value D_α at a 95% significance level
 269 is given as:

$$D_\alpha = 1.36 \sqrt{\frac{1}{n_1} + \frac{1}{n_2}} \quad \text{Eq. 4}$$

270 Where: The 1.36 value is obtained from the Kolmogorov-Smirnov table ([Massey](#)
 271 [Jr 1951](#)). n_1 and n_2 are the sizes of sample 1 and sample 2 respectively.

272 The null hypothesis is: both samples come from a population with the same
 273 distribution. The null hypothesis is retained at significance level α if $D^* < D_\alpha$.
 274 However, when the sample size is too large (e.g. $n \geq 900$), the null hypothesis
 275 would be constantly rejected because its corresponding critical value D_α would
 276 be very small. In other words even extremely small difference between the
 277 estimate and the null hypothesis can be statistically significant (p – values < 0.05)
 278 ([Lin, Lucas Jr and Shmueli 2013](#)). To illustrate this ‘large-sample, small p -values’
 279 problem, Monte Carlo simulation was introduced into K-S test when testing
 280 whether two sample come from the same distribution. The detailed procedure is
 281 described in Table 2.

Table 2 Algorithm for illustrating ‘large-sample, small p -values’ problem in K-S test

-
1. Select two fleets, randomly sample n data points ($n = n_1 = n_2 = 100$) from each fleet, apply K-Stest to generate the maximum difference $D_{100(1)}^*$ between these 2 fleets
 2. Repeat step 1 for 1000 times, D_{100}^* can be obtained as $\{D_{100(1)}^*, D_{100(2)}^*, \dots, D_{100(1000)}^*\}$
 3. Identify the theoretical distribution of $D_{(100)}^* \{D_{100(1)}^*, D_{100(2)}^*, \dots, D_{100(1000)}^*\}$, estimate the typical value of D_{100}^* based on the distribution
 4. Compare the typical value of D_{100}^* with its corresponding critical value D_α
 5. Increase the last sample size n by 100, ($n_1 = n_2 = n = 200, 300, \dots, 1200$), repeat step 1-5 until the sample size n gets to 1200
-

282 Data from the Belgium and Switzerland Euro 6a/b class III fleets were taken as
 283 an example to demonstrate the relationship between sample size and test results.
 284 Figure 3-a shows the median value of D^* (the black line in each boxplot) is higher
 285 than its corresponding D_α value (the red line) when $n \geq 900$, and Figure 3-b
 286 shows p -value is constantly below 0.05 when $n \geq 900$. In other words, the null

287 hypothesis would be constantly rejected when the sample size n is larger than or
288 equal to 900.

289 Figure 3-a shows the median D^* value is stable when the sample size $n \geq 500$.
290 To avoid the 'big sample' issue, a Monte Carlo simulation at a sample size of 500
291 was applied on K-S test when testing if two fleets are likely from the same
292 distribution and can be combined to one. As D^* follows a lognormal distribution
293 ([Wang, Zeng and Shao 2011](#)), the mode value of D^* is compared with its
294 corresponding D_α . Once confirmed that data from the two countries follow the
295 same distribution, the two data subsets are combined and compared with the next
296 country's data.

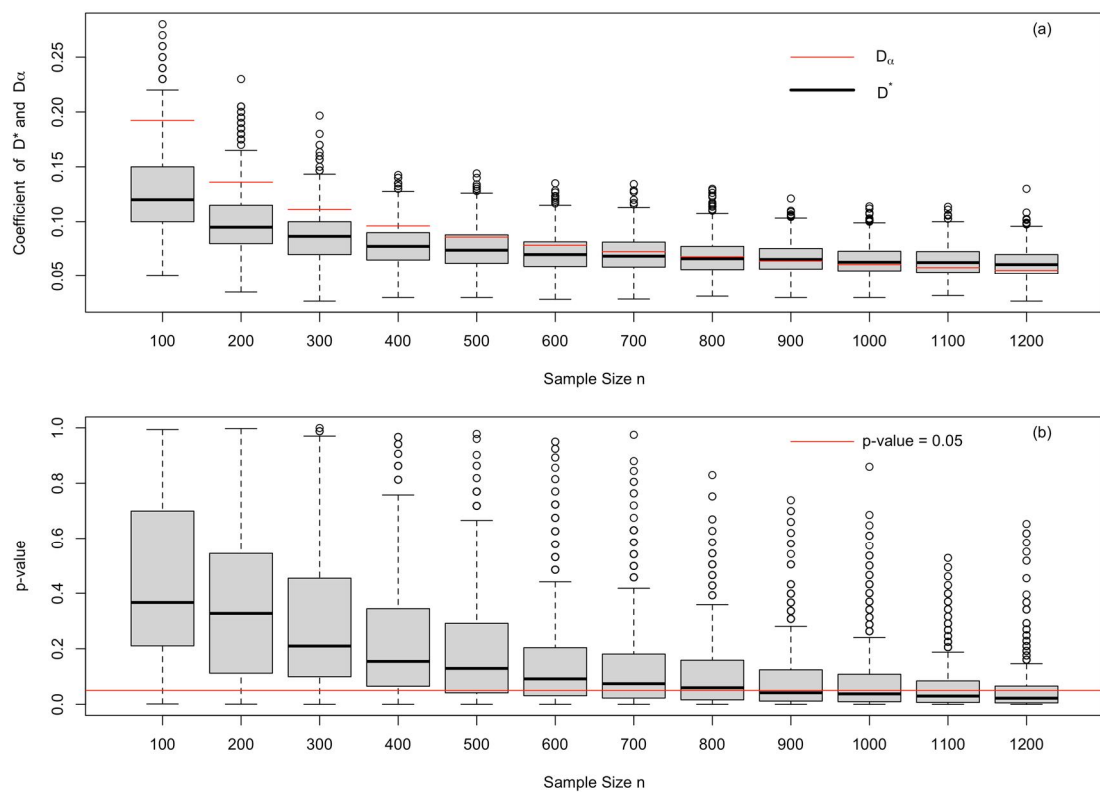


Figure 3 Distribution of (a) D^* [top panel] and (b) p -value [bottom panel] as a function of sample size n

298 **3.1 Comparison of van emission performance in four countries**

299 The algorithm listed in Table 1 has been applied to each Euro standard and class
 300 type across four countries to identify candidate high-emitting ('off-model')
 301 vehicles and estimate the emission performance of normally behaving vehicles
 302 ('on-model') in each fleet. 'Off-model' percentage, 'on-model' vehicles' location
 303 and scale parameters derived from the fitted distributions for each fleet are
 304 documented in Table 3. An illustrative class III Euro 5 and Euro 6a/b fleets' R^2
 305 value plot for each cut-off percentile is shown in Figure 4.

Table 3 'Off-model' percentage and Gumbel distribution fit parameters of 'on-model' vehicles in Belgium, Switzerland, Sweden and the UK

	Country	class II				class III			
		E3	E4	E5	E6a/ b	E3	E4	E5	E6a/ b
'Off-model' percentage	BE	0%	1%	1%	2%	1%	1%	1%	1%
	CH	0%	0%	0%	36%	0%	0%	0%	21%
	SE	NA	0%	1%	8%	NA	0%	1%	3%
	UK	1%	0%	0%	3%	1%	1%	0%	4%
Location (g/kg)	BE	9.25	7.98	8.82	3.34	10.66	9.00	10.66	3.23
	CH	15.24	10.18	13.88	1.32	17.57	12.91	13.98	1.95
	SE	NA	9.96	12.60	2.72	NA	10.81	12.33	2.83
	UK	13.91	11.38	14.09	3.94	14.29	10.64	14.16	3.01
Scale (g/kg)	BE	5.61	5.90	6.62	4.31	6.90	6.45	7.92	4.40
	CH	7.97	7.62	9.65	2.17	9.93	8.67	10.07	2.47
	SE	NA	8.81	9.68	4.30	NA	8.66	10.43	4.92
	UK	8.67	9.25	9.67	5.31	11.24	8.69	10.13	4.62

306 The majority of the Euro 3, Euro 4 and Euro 5 van fleets follow the Gumbel
 307 distribution, with only 1% or 0% of 'off-model' vehicles identified in these fleets.
 308 The explanation for this is that the bulk of the Euro 3~5 diesel vans have high
 309 emissions, so the measurements are fitted to Gumbel distributions with relatively
 310 high location and scale parameters, as also reported for diesel cars by [Rushton,
 311 Tate and Shepherd \(2021\)](#). For Euro 6a/b vans, more outliers have been
 312 identified, with 'off-model' shares ranging from 1% to 8% for Belgium, Sweden
 313 and the UK, while Switzerland is identified to have 36% and 21% 'off-model'
 314 vehicles for class II and class III respectively. The majority of the Euro 6a/b fleet
 315 of vehicles are relatively clean in comparison with their predecessors, with a
 316 proportion of outliers that cannot be fitted into the Gumbel distribution and are
 317 therefore regarded as candidate high-emitting ('off-model') vehicles. The steep
 318 road grade at the Swiss monitoring sites is proposed as an explanation for the

319 high share of candidate high-emitting ('off-model') in the Euro 6a/b fleet detected
320 at these sites, and the details are provided in section 3.2.

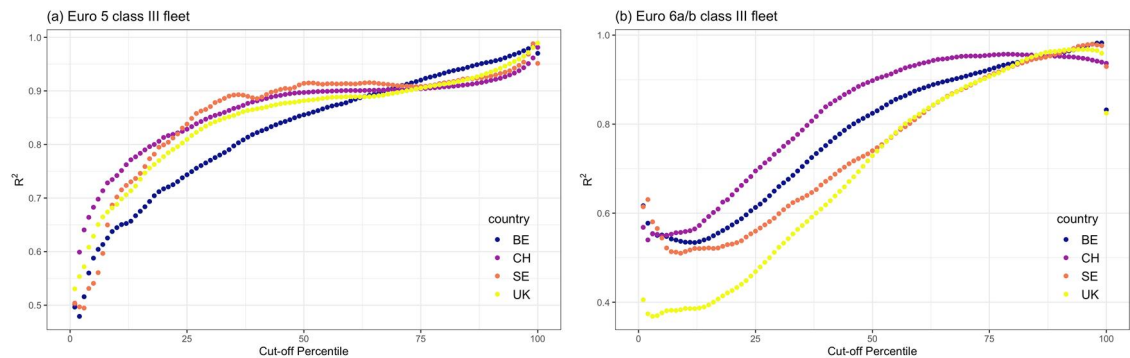


Figure 4 Variation in R^2 value as a function of cut-off percentile for (a) Euro 5 class III diesel vans [left]; (b) Euro 6a/b [right] class III diesel vans

321 The location parameter of Euro 3, 4, 5 and 6ab 'on-model' vehicles in the four
322 countries are shown in Figure 5 i.e. the emission rates that have been recorded
323 with the highest frequency in the deemed normally behaving fleet. The results for
324 the four countries follow broadly the same trend, with the NO_x emission
325 performance of typical vans remaining broadly stable through Euro standards 3
326 to 5, with emissions from Euro 5 vans slightly higher than their Euro 4
327 predecessors. These findings are in-line with other studies ([Chen and Borken-](#)
328 [Kleefeld 2014](#); [ICCT 2019a](#)). There is observed to be a significant improvement
329 for Euro 6a/b, with an average 76.4% decrease in the fleet weighted location
330 parameter for class III Euro 6a/b vehicles over Euro 5. The Euro 6 emission
331 standard is more stringent with regard to the limit of NO_x (declines from 0.28 g/km
332 (Euro 5) to 0.125 g/km (Euro 6a/b) for class III diesel vans, a reduction of 55%⁶).
333 The implementation of Euro 6 is also directing manufactures to use more effective
334 after-treatment system for NO_x emissions, such as selective catalytic reduction
335 (SCR), lean NO_x trap (LNT), and exhaust gas recirculation (EGR). The integration
336 of these NO_x control systems is observed to be leading to a considerable
337 reduction in real-world NO_x emissions. The scale parameter fitted to Euro 6a/b is
338 also approximately half that of Euro 5 vans' (see Table 3), demonstrating that
339 there is not only a significant decrease in the typical NO_x emission rates, but also
340 that the emission rates in this sub-fleet are becoming more centralized
341 (consistent).

342 Test conditions (road grade, ambient temperature and VSP) have been found
343 important to diesel van emission performance. NO_x emissions of Euro 3 to 5
344 vehicles in Switzerland are relatively high as the remote sensing campaigns

⁶ Regulation (EC) 715/2007

345 carried out during 2011 to 2015 were at a site with a steep road grade (9%), and
 346 higher road grade is known to elevate NO_x emissions ([Costagliola, Costabile and](#)
 347 [Prati \(2018\)](#)). The Euro 6a/b ‘on-model’ van emissions in Switzerland are however
 348 low in comparison with other countries, on account of only two third of the vehicles
 349 are regarded as ‘on-model’ vehicles (reason discussed in section 3.2). The typical
 350 NO_x emissions of Euro 5 and Euro 6a/b in the UK are considered relatively high
 351 and it may be associated with their low ambient temperatures. Remote sensing
 352 campaigns carried out in the UK in 2017 and 2018 were in wintertime (around
 353 10°C), during which 63% and 100% of Euro 5 and Euro 6a/b vehicles were
 354 measured. Studies ([Sjödin et al. 2017](#); [Grange et al. 2019](#); [ICCT 2019a](#)) have
 355 found out that light-duty diesel NO_x emissions are highly dependent on ambient
 356 temperature, with low temperature elevating NO_x emissions. However, these
 357 studies also indicate that the temperature dependence is significant for Euro 5
 358 and Euro 4, but less so for Euro 6a/b fleet. Belgium has relatively low NO_x
 359 emissions despite its high VSP values and high certificated CO₂ emissions. The
 360 Belgium measurements were all made on a highway with an average vehicle
 361 speed of more than 70km/h, hence high VSP levels for drive-through
 362 measurements associated with aerodynamic drag and rolling resistance at these
 363 speeds. This finding is also observed in PEMS tests of Euro 5 and Euro 6a/b
 364 diesel cars, where vehicles in motorway driving conditions emit less NO_x than
 365 those on sections of urban areas ([O’Driscoll et al. 2018](#)). It is hypothesised that
 366 high and sustained speed would also provide enough temperature for the NO_x
 367 emission control system (e.g. EGR and SCR) commonly deployed to maintain
 368 their high efficiency operating temperature ([Yang et al. 2021](#); [Ntziachristos et al.](#)
 369 [2016](#)).

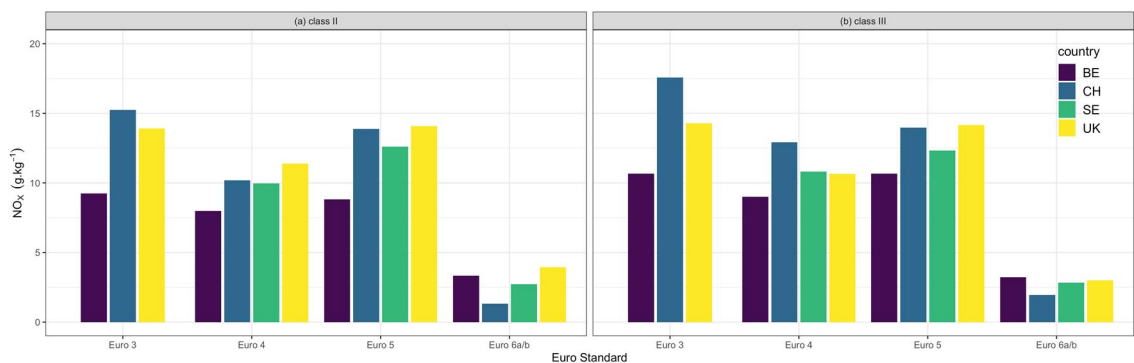


Figure 5. Typical NO_x emission rates (g/kg) for normally behaving (a) class II [left] and (b) class III [right] diesel vans by Euro standard and country

370 **3.2 Impact of road grade on candidate high NO_x emitting vans**

371 Recent remote sensing campaigns in Switzerland (year 2016~2019) were carried
372 out at six sites with road grades ranging from 2.4% to 9.4%. It is hypothesised
373 that the high percentage of 'off-model' vehicles found in Swiss Euro 6a/b fleet
374 may be related to the steep road grade at some of the campaign sites. Data from
375 Euro 6a/b class II and class III fleet in the Switzerland are classified by road grade
376 and Gumbel distributions fitted and 'off-model' fractions estimated using the
377 maximum R^2 value method (see Table A. 3 in the Appendix). The results illustrate
378 that sites with steeper road grade (4.4% and 9.4%) have a much higher
379 percentage of 'off-model' vehicles, which may partly explain why there are more
380 'off-model' vehicles identified in the Swiss Euro 6a/b fleet.

381 Figure 6 presents the 'on-model' vehicles in Euro 6a/b class II and class III fleets
382 (see the orange triangular dots in Figure 6-a and Figure 6-b). NO_x emission rates
383 in sites with relatively gentle slopes (site 1, site 2 and site 3) are higher than uphill
384 sites (site 4, site 5 and site 6). The trend is contrary to findings for Euro 5 vehicles
385 (refer to the blue triangular dots in Figure 6-a and Figure 6-b), where higher road
386 grade would lead to elevated NO_x emissions ([Costagliola, Costabile and Prati 2018](#)).
387 This is considered to be because SCR system equipped on Euro 6a/b
388 vans can achieve better NO_x reductions when the exhaust temperature is high
389 enough ([Moody and Tate 2017](#)). When Euro 6a/b vehicles are driven on steep
390 road grade site, the consequent high engine load would result in better effective
391 conversions and catalytic reductions in the SCR system and that may offset the
392 emission increase caused by higher engine load (higher road grade).

393 [Rushton, Tate and Shepherd \(2021\)](#) found that candidate high-emitting vehicle
394 sub-fleets also follow the Gumbel distribution, so vans being classified as 'off-
395 model' vehicles in Swiss Euro 6a/b fleet are also fitted to the Gumbel distribution
396 (results documented in Table A. 3 in the Appendix). The location value of each
397 sub-fleet are regarded as the typical NO_x emission rates of the high emitting
398 vehicles, and illustrated as orange circle dots in Figure 6-a and Figure 6-b (Euro
399 5 fleet doesn't have 'off-model' vehicles). In steep road grade (4.4% and 9.4%),
400 the difference between 'on-model' vehicles and 'off-model' vehicles for Euro 6a/b
401 class II vehicles is larger than Euro 6a/b class III vehicles. The results therefore
402 suggest that the NO_x performance of class II Euro 6a/b vans deemed high-
403 emitters are more sensitive to road grade compared with their class III
404 counterparts. Considering these class II and class III fleets were measured in the
405 same driving conditions, the difference in emission performance may be caused
406 by different vehicle characteristics and performance of their respective exhaust
407 after-treatment systems. However, based on the vehicle make/model information
408 in the remote sensing database and further after-treatment system information

409 (documented in Table A. 4 in the Appendix) extracted from the ADAC⁷ vehicle
 410 catalogue or corresponding van brochures, it is found that the almost all popular
 411 models (the top-ten most commonly observed) in Euro 6a/b class II and class III
 412 vans in Switzerland are equipped with SCR systems, so the relatively poorer
 413 emission characteristics of class II vans is not found to be attributed to the type
 414 of after-treatment technology, rather their performance in the driving
 415 characteristics at this site. Further analysis of the difference between class II and
 416 class III in Euro 6a/b fleets is conducted in the next section.

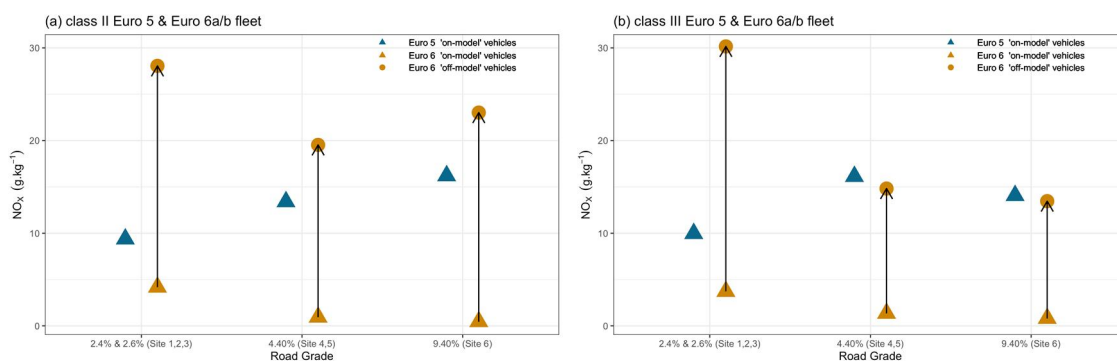


Figure 6 Impact of road grade on the typical NO_x emission rates (g/kg) of ‘on-model’ and ‘off-model’ vehicles as a function of road grade in Switzerland for sub-fleets (a) class II Euro 5 & Euro 6a/b [left]; (b) class III Euro 5 & Euro 6a/b [right] (note there are no ‘off-model’ vehicles in Euro 5 fleet)

417 It’s more likely that these ‘off-model’ vehicles only temporarily emit high rates of
 418 NO_x at sites with steep uphill road gradients, rather than they are indeed high-
 419 emitters and can be more effectively identified on a steeper road, otherwise the
 420 same percentage of ‘off-model’ vehicles would probably be identified at other
 421 sites with lower road grade. Accordingly, if the purpose is to have an emission
 422 evaluation of typical vehicles in more normal operating conditions, it is advised
 423 that remote sensing campaigns be conducted at sites with a gentle slope.

424 **3.3 The NO_x performance of normally behaving Euro 6a/b vans** 425 **by vehicle model and manufacture group**

426 To further investigate Euro 6a/b vans’ emission performance, remote sensing
 427 data can be segmented by models or manufacturing groups (“families”) ([ICCT](#)
 428 [2019a](#)). However, further breaking down the fleets within one country and
 429 analysing its characteristics will not derive any useful conclusion as the sample
 430 size is too small, rather the remote sensing data across different countries needs

⁷ <https://www.adac.de/>

431 to be combined together. To test if the four countries' data can be merged into
 432 one bigger dataset, a two sample K-S test explained in section 2.4 is applied. The
 433 result shows that for Euro 6a/b class II vans' remote sensing measurements:
 434 Belgium, Sweden and the UK follow the same distribution and can be combined
 435 into a single dataset. For Euro 6a/b class III vans' remote sensing measurements:
 436 all four countries are found to be from the same distribution and can be combined
 437 to a single dataset. After combining data from three countries in class II fleet and
 438 four countries in class III fleet, the Gumbel distribution and maximum R^2 method
 439 is applied to two fleets. A 4% of 'off-model' vehicles is found for each fleet. For
 440 class II Euro 6a/b vans, the 4% 'off-model' vehicles accounts for 24% of total NO_x
 441 emission, while the 4% 'off-model' vans in Euro 6a/b class III fleet accounts for
 442 21% of total NO_x emission. The Gumbel distribution fitted to both the 'on-model'
 443 and 'off-model' vehicles is documented in see Table 4. The typical emission rate
 444 (location value) for class II vans are slightly higher than class III vans, with a
 445 greater spread in the distribution (higher scale value). When analysing the vehicle
 446 characteristics, no significant difference is found between 'on-model' and 'off-
 447 model' vans (shown in Table 4), except that the average engine size of class II
 448 'off-model' vans is lower than the 'on-model' vans.

Table 4 Gumbel distribution fit parameters and fleet characteristics of 'on-model' and 'off-model' vans in merged Euro 6a/b dataset

	Class II (BE, SE, UK)		Class III (BE, CH, SE, UK)	
	'On-model'	'Off-model'	'On-model'	'Off-model'
Sample size (n)	5120	214	15777	658
Location parameter(g/ kg)	3.30	33.24	3.00	29.36
Scale parameter (g/ kg)	4.50	5.87	4.33	4.34
Fit R^2	97.51%	97.97%	97.23%	97.98%
Vehicle age (year)	1	1	1	1
Certificated CO_2 emission (g/ km)	130	131	185	184
Engine size (cm^3)	1698	1554	2106	2083
Rated power (kW)	77	76	107	105
Curb weight (kg)	1505	1493	2139	2169

449 Engine downsizing is a technology to improve fuel efficiency for lighter vehicles
 450 by reducing the frictional losses and relative weight of the engine (and total kerb-
 451 weight), while the turbocharger helps provide the levels of power demanded

452 (Manzie 2010). While reducing CO₂ emissions, a downsized diesel engine is
453 found to increase NO_x (Johnson 2009). Payri et al. (2014) assesses the diesel
454 engine downsizing limitation related to heat losses and turbocharger efficiency
455 reduction, which suggests it might be associated with excessive emissions.
456 However, there is no research related to engine downsizing problem of Euro 6a/b
457 light-duty vehicles.

458 To test whether engine size has an impact on NO_x emissions, the merged class
459 II and class III fleet are split into different sub-fleet by models and makes. Table
460 A. 5 in the Appendix listed the top 5 popular models for class II and class III Euro
461 6a/b vans, and its corresponding Gumbel distribution fit parameters for the 'on-
462 model' vehicles, as well as every model's engine size and vehicle rated power.
463 All the models listed are equipped with SCR after-treatment system⁸, which
464 indicates that the type of NO_x control system is not the reason for the different
465 emission performance between models. kW/litre specific power is introduced to
466 represent the power density, with a higher kW/litre being characteristic of a
467 downsized engine. Figure 7 demonstrates that the kW/litre specific power of top
468 5 models in class II Euro 6a/b fleets are more spread over compared with models
469 in class III fleets. Transit Connect with the highest kW/litre specific power in class
470 II fleet has much higher NO_x emissions. However, that's not the case for large
471 class III Euro 6a/b vans, where both NO_x emissions and the kW/litre specific
472 power of class III Euro 6a/b vans are relatively stable.

473 It is suspected that when the engine gets too small relative to the vehicle size and
474 weight, and is driven in a relatively aggressive manner, the engine turbo-charging
475 may not be capable of maintaining the engine power, resulting in worse fuel
476 economy and NO_x emissions. Given the complexity of engine specifications,
477 further investigation is required by conducting additional laboratory tests to fully
478 appreciate the reasons behind the suspected excessive NO_x emissions from
479 engine down-sizing. During the test NO_x emissions will be measured using a
480 constant volume sampling system connecting with a gas analyser while engine
481 load being tested in an engine test bench (Gao et al. 2019).

⁸ <https://www.adac.de/>

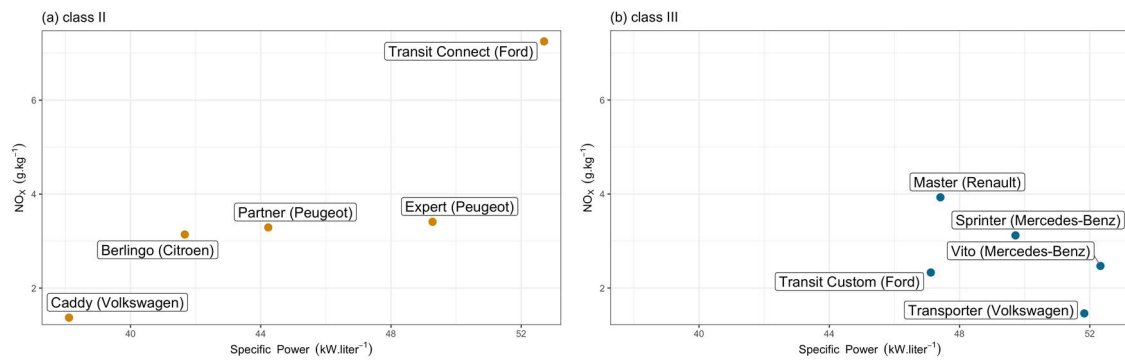


Figure 7 Relationship between kW/litre specific power and NO_x emissions (g/kg) for popular models in Euro 6a/b merged fleet: (a) class II [left]; (b) class III [right]

482 Merged class II and class III Euro 6a/b diesel vans are also segmented by
 483 manufacture groups, and then applied to the Gumbel distribution and maximum
 484 R^2 value cutting method. Table A. 6 in the Appendix lists 8 popular manufacture
 485 groups and their respective brands, which cover over 98% of the remote sensing
 486 measurements. Table A. 7 in the Appendix lists the detailed results of the Gumbel
 487 distribution fit parameters of ‘on-model’ vehicles for all the popular manufacture
 488 groups. Figure 8 presents the fuel-specific NO_x emissions of ‘on-model’ vehicles
 489 in each manufacture group, ordered by descending NO_x emissions. The width of
 490 the bar is the corresponding sample size of a specific manufacture group.

491 For the most part, manufacture group performance of class III vans is in line with
 492 the [ICCT \(2019a\)](#) report, as the number of class III vans outnumber class II vans
 493 by 3 times. The emission contribution from Class III van therefore dominates the
 494 overall trend of the van fleet. NO_x emissions vary considerably by manufacture
 495 group, and even within the same manufacture group between the performance
 496 of class II and class III vans. Daimler and Ford are found to have the worst NO_x
 497 emission performance in class II vehicles, while their class III vehicles emissions
 498 are within the average range. On the other end of the scale, the PSA Group
 499 vehicles are relatively clean in class II vehicles but are identified as the third-
 500 highest emitting manufacture in class III vehicles. The VW Group is the
 501 manufacture with cleanest NO_x emission performance of both class II and class
 502 III vehicles.

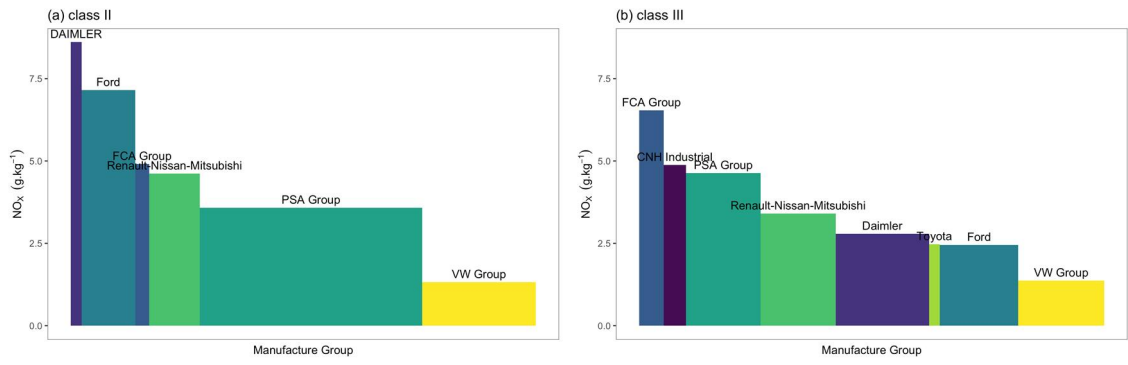


Figure 8 NO_x emissions (g/kg) by popular manufacture groups in Euro 6a/b merged fleet: (a) class II [left]; (b) class III [right] (the width of the bar is the corresponding sample size)

503 4 Summary and conclusions

504 The distribution of diesel van fuel-specific NO_x emissions in g/kg measured by
505 remote sensing is skewed-right. To accurately characterize van emission
506 performance and find the cut-off point for candidate high-emitters, the Gumbel
507 distribution is applied to vehicle emission remote sensing data from four
508 countries. Vehicles that follow the Gumbel distribution are selected to represent
509 the emission performance of the normally behaving vehicles in a fleet, while the
510 vehicles that do not follow the Gumbel distribution are regarded as candidate high
511 emitting vehicles. Euro 5 and older vehicles can be fully described by the Gumbel
512 distribution while a proportion of candidate high-emitters are identified in the Euro
513 6a/b fleets. The emphasis of this paper is examining the emission performance
514 of the normally behaving vehicles and candidate high-emitters in Euro 6a/b fleet,
515 and the key findings are:

- 516 • When comparing the fuel-specific NO_x emissions of the normally behaving
517 vans, a reduction of emissions has only been seen since the introduction
518 of Euro 6a/b standard vehicles, where the emissions is less than one third
519 of the emissions from Euro 5 vans.
- 520 • A much higher percentage of 'off-model' Euro 6a/b vans has been
521 observed at the measurement sites in Switzerland that had a steeper road
522 grade, and it's more likely that vehicles at these sites only temporarily emit
523 high rates of NO_x. Based on this it is recommended to conduct remote
524 sensing campaigns at a site with a gentle slope, so the assessment of the
525 vehicles' emission performance surveyed is in typical driving/operating
526 conditions across a city/region/country.
- 527 • Euro 6a/b vans with improved NO_x after-treatment system (e.g. SCR) can
528 offset the emission increasing caused by high VSP or steep road grade,
529 as high engine load can provide enough exhaust emission temperature for
530 the after-treatment system to work efficiently.
- 531 • After combining data from three countries in class II fleet and four countries
532 in class III fleet, a consistent 4% of candidate high-emitters are found in
533 both class II and class III merged Euro 6a/b vans, estimated to account for
534 24% and 21% total NO_x emissions respectively.
- 535 • Differentiating the cross-country merged data by models and analysing the
536 relationship of kW/litre and emissions, illustrates that Euro 6a/b Class II
537 vans are more sensitive to engine size. Rather than attributing the reason
538 to different application and design of emission after-treatment systems, it's
539 considered more likely to be due to the engine downsizing of smaller class
540 II vans.

- 541 • The merged data are also segmented by manufacture group. The VW
542 Group is identified as the manufacture with the cleanest emission
543 performance in both class II and class III Euro 6a/b vehicles. Daimler and
544 FCA Group emit most in class II and class III Euro 6a/b fleet respectively.

545 This paper analyses the real-world emission performance of diesel Euro 6a/b
546 vans, whose type approval test were being conducted under the NEDC drive
547 cycle. The NEDC drive cycle has many cruise and mild acceleration driving
548 conditions, which cannot represent the more dynamic driving that occur when
549 vehicles are recorded by remote sensing device. To establish a more
550 representative pollution test for light-duty vehicles (cars and vans), a new real-
551 driving emissions (RDE) test procedure was introduced in 2017, and will apply to
552 all new vans by the beginning of 2022⁹. [ICCT \(2019a\)](#) found the vast majority of
553 remote sensing measurements are within normal operating conditions defined in
554 the European RDE regulation. As a result the new Euro 6d-temp and Euro 6d
555 vans with on-road testing are expected to have lower NO_x emissions where
556 emission control systems can operate properly. It is recommended the analytical
557 approach presented in this to identify candidate high-emitters is applied to
558 emerging remote sensing datasets that have significant shares of Euro 6d-temp
559 and Euro 6d vans, to ascertain whether this generation of vehicles have
560 consistently low NO_x emissions, or whether a share of these vehicles with poorer
561 emission performance make a substantial contribution to the total emissions from
562 this sub-fleet.

563 The EU has founded a project called CARES¹⁰ focusing on using contactless and
564 un-intrusive technologies to monitor and enforce improvements in road vehicle
565 emissions, this includes the application of roadside sampling (remote sensing
566 and point sampling devices) and plume chasing ([Pöhler et al. 2019](#)). In the future,
567 measurement data from a remote sensing device may communicate with other
568 systems and technologies¹¹ for market surveillance and enforcement purposes,
569 working towards maintaining a fleet that are in compliance with emission
570 standards. It is suggested the Gumbel distribution could help to characterize the
571 emission performance of the normally-behaving vehicles as well as screen high-
572 emitting vehicles. At local levels, authorities could use the Gumbel distribution to
573 determine the 'cut-points' that will help to identify high-emitting vehicles and clean
574 vehicles. For example, a single, high instantaneous recording may not
575 necessarily mean a vehicle consistently emits at an excessive rate but if a vehicle
576 has two remote sensing recordings above threshold, it may be identified as a

⁹ Commission Regulation (EU) 2017/1151

¹⁰ <https://cordis.europa.eu/project/id/814966>

¹¹ <https://cares-project.eu/>

577 candidate high-emitter and further investigated by plume chasing ([Pöhler et al.](#)
578 [2019](#)) and/or the registered keeper is directed to get the vehicle tested at an
579 authorized emission testing centre such as garage inspection ([Huang et al. 2018](#)).
580 At a state level, the government could use the Gumbel distribution to characterize
581 the emission performance of a vehicle family, and identify high-emitting vehicle
582 manufactures or models.

583 **Acknowledgements**

584 This study has benefited greatly from the use of the CONOX db ([Borken-Kleefeld](#)
585 [et al. 2018a](#)). The CONOX project focusing on pooling, sharing, and analysing
586 European remote sensing data collected in a range of European cities. The
587 authors would like to acknowledge the support from the CARES project (H2020
588 Grant Agreement no 814966). The authors are grateful to Åke Sjödin (IVL
589 Sweden), BORKEN-KLEEFELD Jens (IIASA Austria) and Stefan Hausberger
590 (TU Graz Austria), for providing their insightful comments on our manuscript.
591 Zhuoqian Yang acknowledges the support of the Great Britain-China Educational
592 Trust.

5 Appendix A. Supplementary data

Table A. 1 Summary of remote sensing fleet characteristics and test conditions in Belgium, Switzerland, Sweden and the UK

	Country	Class I				Class II				Class III			
		E3	E4	E5	E6a/ b	E3	E4	E5	E6a/ b	E3	E4	E5	E6a/ b
Fleet characteristics													
Measurement instrument and year	BE	EDAR: 2019											
	CH	RSD 4600: 2011~2015; RSD 5000: 2016~2019											
	SE	RSD 5000: 2016, 2018											
	UK	RSD 4600: 2013,2015; RSD 5000: 2017,2018; FEAT: 2012,2013,2017,2018											
Sample size(n)	BE	106	414	484	434	263	1016	2257	2700	389	2040	7812	7361
	CH	137	135	122	164	576	1288	2427	883	3894	9956	16616	4233
	SE	12	24	22	NA	91	243	1035	1212	132	422	1772	1919
	UK	305	866	1513	201	599	3478	7030	1422	392	3227	12098	2940
Average vehicle age (years)	BE	15	10	5	1	14	10	5	1	15	10	5	1
	CH	13	10	4	2	12	8	5	2	13	8	5	2
	SE	12	7	4	NA	12	7	3	1	12	7	3	1
	UK	9	6	3	1	9	6	3	1	9	6	3	1
Certificated CO2 emission (g/ km)	BE	146	135	121	113	210	183	149	132	252	228	207	186
	CH	154	136	117	115	147	158	140	129	221	234	212	185
	SE	NA	131	111	NA	155	151	140	118	232	226	204	173
	UK	128	129	122	101	155	168	156	130	219	219	207	184
Test conditions													
Ambient temperature (°C)	BE	22.5	22.7	23.0	22.2	22.5	22.6	22.9	23.2	22.5	22.5	22.9	23.0
	CH	22.8	21.2	23.6	24.5	20.7	22.3	23.4	25.1	21.2	22.0	23.4	25.2
	SE	19.2	19.9	22.9	NA	20.4	19.4	19.6	21.2	21.7	21.4	20.7	21.6

	UK	17.1	14.2	12.1	10.5	17.9	14.6	11.5	10.3	17.2	14.1	11.4	10.2
Road grade (%)	BE	2.0	2.0	2.0	2.0	1.9	2.0	2.0	2.0	1.9	2.0	2.0	2.0
	CH	8.0	7.8	6.0	8.9	8.6	7.5	6.5	4.8	8.5	7.7	6.5	4.5
	SE	3.6	3.6	3.1	NA	3.3	3.3	3.3	1.6	3.2	3.2	3.2	1.2
	UK	2.6	2.2	2.1	1.4	2.4	2.3	1.9	1.8	2.4	2.0	1.8	1.6
VSP (kW/ton)	BE	18.8	15.1	14.4	16.3	16.1	17.2	16.0	15.4	15.2	17.6	15.5	15.6
	CH	16.6	15.7	14.7	17.7	15.5	14.8	14.2	12.6	15.5	14.7	13.7	11.6
	SE	9.4	12.5	11.0	NA	11.1	10.6	10.7	12.0	10.1	11.7	10.6	12.0
	UK	9.0	8.8	8.4	11.4	7.9	7.6	7.9	9.0	7.3	7.1	8.1	8.5

Table A. 2 The fraction of primary NO₂ in NO_x (f_{NO2}) by Euro standard and class type

	Class I	Class II	Class III
Euro 3	12.96%	11.36%	13.53%
Euro 4	27.94%	25.68%	28.12%
Euro 5	25.25%	21.06%	19.10%

Table A. 3 Gumbel distribution fit parameters and VSP values for ‘on-model’ and ‘off-model’ Euro 6a/b and Euro 5 vehicles by road grade in Switzerland

Road grade and Site	Class II					Class III				
	Off-model percentile	Vehicle status	Sample size (n)	NO _x (g/ kg)	VSP (kW/ ton)	Off-model percentile	Vehicle status	Sample size (n)	NO _x (g/ kg)	VSP (kW/ ton)
	Euro 6a/ b									
2.2% & 2.4% (site 1,2,3)	11%	‘On-model’	215	4.18	9.8	2%	‘On-model’	728	3.72	9.0
		‘Off-model’	26	28.06	11.7		‘Off-model’	15	30.16	9.4
4.4% (site 4,5)	30%	‘On-model’	245	0.94	11.0	32%	‘On-model’	1623	1.36	11.8
		‘Off-model’	105	19.53	13.0		‘Off-model’	764	14.82	11.6
9.4% (site 6)	45%	‘On-model’	95	0.46	17.3	16%	‘On-model’	318	0.81	16.3
		‘Off-model’	78	23.02	19.2		‘Off-model’	61	13.46	15.7
	Euro 5									
2.2% & 2.4% (site 1,2,3)	0%	‘On-model’	387	9.38	9.6	0%	‘On-model’	2058	9.97	8.8
4.4% (site 4,5)	0%	‘On-model’	555	13.4	12.3	0%	‘On-model’	4795	16.13	11.9
9.4% (site 6)	0%	‘On-model’	1146	16.2	16.8	0%	‘On-model’	7220	14.07	16.3

Table A. 4 Popular models in Swiss Euro 6a/b class II and class III vans and corresponding after-treatment system information

Class II			Class III		
Model (make)	Sub-fleet Share	Equipped with SCR or not	Model (make)	Sub-fleet Share	Equipped with SCR or not
Caddy (Volkswagen)	40.32%	SCR	Transporter (Volkswagen)	14.85%	SCR
Kangoo (Renault)	11.33%	SCR	Vito (Mercedes-Benz)	12.10%	SCR
Transit Connect (Ford)	9.97%	SCR	Transit Custom (Ford)	10.19%	SCR
Partner (Peugeot)	7.25%	SCR	Trafic (Renault)	9.39%	SCR
Nv200 (Nissan)	5.89%	No SCR	Daily (Iveco)	6.15%	Some with SCR, some not
Doblo (Fiat)	5.66%	SCR	Master (Renault)	5.58%	SCR
Citan (Mercedes-Benz)	4.42%	No SCR	Crafter (Volkswagen)	5.25%	SCR
Combo (Opel)	4.19%	SCR	Ducato (Fiat)	5.22%	SCR
Berlingo (Citroen)	2.94%	SCR	Vivaro-B (Opel)	4.96%	SCR
Proace (Toyota)	2.15%	SCR	Transit (Ford)	2.86%	SCR

Table A. 5 ‘On-model’ Gumbel distribution fit parameters and fleet characteristics by top 5 Euro 6a/b models

	Model (make)	Sample size (n)	Sub-fleet share	Off-model percentile	Fit R^2	Location (g/ kg)	Scale (g/ kg)	Engine size (cm ³)	Engine power (kW)
Class II	Caddy (Volkswagen)	1267	21.97%	1%	98.77%	1.37	2.96	1968	75
	Partner (Peugeot)	782	13.56%	2%	98.07%	3.29	4.55	1560	69
	Berlingo (Citroen)	694	12.04%	1%	97.40%	3.14	4.52	1560	65
	Transit Connect (Ford)	582	10.09%	2%	98.54%	7.25	6.80	1499	79
	Expert (Peugeot)	423	7.34%	1%	99.28%	3.41	4.31	1867	92
Class III	Transit Custom (Ford)	1812	10.79%	3%	96.86%	2.33	4.42	1995	94
	Transporter (Volkswagen)	1573	9.36%	8%	97.25%	1.46	3.17	1968	102
	Sprinter (Mercedes-Benz)	1554	9.25%	1%	98.96%	3.12	3.95	2293	114
	Vito (Mercedes-Benz)	1358	8.08%	4%	98.08%	2.47	3.40	2064	108
	Master (Renault)	1207	7.18%	1%	97.63%	3.93	5.08	2299	109

Table A. 6 List of manufacturer groups and brands

Manufacture Group	Make Name	Manufacture Group	Make Name
CNH Industrial	Iveco	PSA Group	Citroen, Opel, Peugeot, Vauxhall
Daimler	Mercedes-Benz	Renault-Nissan-Mitsubishi	Mitsubishi, Nissan, Renault
FCA Group	Fiat	Toyota	Toyota
Ford	Ford	VW Group	Man, Volkswagen

Table A. 7 ‘On-model’ Gumbel distribution fit parameters by popular Euro 6a/b manufacture group

	Manufacture group	Sample size (n)	Off-model percentile	Fit R^2	Location (g/ kg)	Scale (g/ kg)
Class II	PSA Group	2499	1%	98.09%	3.58	4.69
	VW Group	1277	2%	98.74%	1.32	2.90
	Ford	601	2%	98.36%	7.15	6.71
	Renault-Nissan-Mitsubishi	569	7%	97.38%	4.62	5.53
	FCA Group	158	4%	98.25%	4.91	4.53
	DAIMLER	122	1%	97.64%	8.61	8.93
Class III	Daimler	3239	2%	98.50%	2.79	3.76
	VW Group	2985	6%	97.41%	1.37	3.03
	Ford	2721	4%	97.01%	2.45	4.28
	Renault-Nissan-Mitsubishi	2608	3%	96.96%	3.40	4.52
	PSA Group	2583	1%	98.33%	4.63	5.40
	FCA Group	847	1%	98.19%	6.54	6.37
	CNH Industrial	779	1%	97.53%	4.88	6.22
	Toyota	375	12%	97.74%	2.47	3.39

6 Reference

- AWEL. 2019. *Langjährige Abgasmessungen im realen Fahrbetrieb mittels Remote Sensing* [online]. [Accessed 25 March 2020]. Available from: https://awel.zh.ch/content/dam/audirektion/awel/luft_asbest_elektrosmog/verkehr/rsd/dokumente/RSD_Bericht_2018.pdf.
- BEATON, S. P., G. A. BISHOP, Y. ZHANG, L. L. ASHBAUGH, D. R. LAWSON and D. H. STEDMAN. 1995. On-road vehicle emissions: Regulations, costs, and benefits. *Science*, **268**(5213), pp.991-993.
- BHAGAT, N. 2017. Flood frequency analysis using Gumbel's distribution method: a case study of Lower Mahi Basin, India. *Journal of Water Resources and Ocean Science*, **6**(4), pp.51-54.
- BISHOP, G. A., D. A. BURGARD and D. H. STEDMAN. 2006. *On-Road Remote Sensing of Automobile Emissions in the Chicago Area: Year 6, September 2004* [online]. [Accessed 11 June 2021]. Available from: http://www.feat.biochem.du.edu/assets/databases/Illinois/Arlhghts/Chicago_Year_6_CRC2004.pdf.
- BISHOP, G. A. and D. H. STEDMAN. 1996. Measuring the Emissions of Passing Cars. *Accounts of Chemical Research*, **29**(10), pp.489-495.
- BISHOP, G. A., D. H. STEDMAN, D. A. BURGARD and O. ATKINSON. 2016. High-Mileage Light-Duty Fleet Vehicle Emissions: Their Potentially Overlooked Importance. *Environmental Science & Technology*, **50**(10), pp.5405-5411.
- BORKEN-KLEEFELD, J. 2013. *Guidance note about on-road vehicle emissions remote sensing* [online]. [Accessed 11 June 2021]. Available from: https://theicct.org/sites/default/files/publications/RSD_Guidance_BorkKlee.pdf.
- BORKEN-KLEEFELD, J., Y. BERNARD, D. CARSLAW, Å. SJÖDIN, J. TATE, G.-M. ALT, J. DE LA FUENTE, P. MCCLINTOCK, R. GENTALA, S. HAUSBERGER and M. JERKSJÖ. 2018a. *Contribution of vehicle remote sensing to in-service/real driving emissions monitoring - CONOX Task 3 report* [online]. Swiss Federal Office for the Environment (FOEN). [Accessed 14 April 2021]. Available from: <https://www.ivl.se/download/18.34244ba71728fcb3f3fa5b/1591705759730/C295.pdf>.
- BORKEN-KLEEFELD, J. and T. DALLMANN. 2018. *Remote sensing of motor vehicle exhaust emissions* [online]. [Accessed 11 June 2021]. Available from: https://theicct.org/sites/default/files/publications/Remote-sensing-emissions_ICCT-White-Paper_01022018_vF_rev.pdf.
- BORKEN-KLEEFELD, J., S. HAUSBERGER, P. MCCLINTOCK, J. TATE, D. CARSLAW, Y. BERNARD, Å. SJÖDIN, M. JERKSJÖ, R. GENTALA, G.-M. ALT and J. DE LA FUENTE. 2018b. *Comparing emission rates derived from remote sensing with PEMS and chassis dynamometer tests-CONOX Task 1 report* [online]. Swiss Federal Office for the Environment (FOEN). [Accessed 14 April 2021]. Available from: <https://www.ivl.se/download/18.34244ba71728fcb3f3fa59/1591705759529/C293.pdf>.
- BURGARD, D. A., G. A. BISHOP, R. S. STADTMULLER, T. R. DALTON and D. H. STEDMAN. 2006. Spectroscopy Applied to On-Road Mobile Source Emissions. *Applied Spectroscopy*, **60**(5), pp.135A-148A.

- CARSLAW, D., S. BEEVERS, J. TATE, E. WESTMORELAND and M. WILLIAMS. 2011. Recent evidence concerning higher NO_x emissions from passenger cars and light duty vehicles. *Atmospheric Environment*, **45**(39), pp.7053-7063.
- CARSLAW, D., N. J. FARREN, J. BORKEN-KLEEFELD and Å. SJÖDIN. 2019. *Study on the durability of European passenger car emission control systems utilizing remote sensing data* [online]. Swiss Federal Office for the Environment (FOEN). [Accessed 6 August 2020]. Available from: <https://www.ivl.se/download/18.4447c37f16fa0999d1924d0/1580894080250/C387.pdf>.
- CARSLAW, D. and G. RHYS-TYLER. 2013. *Remote sensing of NO₂ exhaust emissions from road vehicles* [online]. [Accessed 11 June 2021]. Available from: https://uk-air.defra.gov.uk/assets/documents/reports/cat05/1307161149_130715_DeFraRemoteSensingReport_Final.pdf.
- CARSLAW, D., M. WILLIAMS, J. TATE and S. BEEVERS. 2013. The importance of high vehicle power for passenger car emissions. *Atmospheric Environment*, **68**, pp.8-16.
- CHEN, Y. and J. BORKEN-KLEEFELD. 2014. Real-driving emissions from cars and light commercial vehicles – Results from 13 years remote sensing at Zurich/CH. *Atmospheric Environment*, **88**, pp.157-164.
- CHEN, Y. and J. BORKEN-KLEEFELD. 2016. NO_x Emissions from Diesel Passenger Cars Worsen with Age. *Environmental Science & Technology*, **50**(7), pp.3327-3332.
- CHEN, Y., R. SUN and J. BORKEN-KLEEFELD. 2020. On-Road NO_x and Smoke Emissions of Diesel Light Commercial Vehicles—Combining Remote Sensing Measurements from across Europe. *Environmental Science & Technology*, **54**(19), pp.11744-11752.
- CHEN, Y., Y. ZHANG and J. BORKEN-KLEEFELD. 2019. When is Enough? Minimum Sample Sizes for On-Road Measurements of Car Emissions. *Environ Sci Technol*, **53**(22), pp.13284-13292.
- COSTAGLIOLA, M. A., M. COSTABILE and M. V. PRATI. 2018. Impact of road grade on real driving emissions from two Euro 5 diesel vehicles. *Applied Energy*, **231**, pp.586-593.
- DAVISON, J., Y. BERNARD, J. BORKEN-KLEEFELD, N. J. FARREN, S. HAUSBERGER, Å. SJÖDIN, J. E. TATE, A. R. VAUGHAN and D. CARSLAW. 2020. Distance-based emission factors from vehicle emission remote sensing measurements. *Science of The Total Environment*, **739**, p139688.
- DEMUYNCK, J., D. BOSTEELS, M. DE PAEPE, C. FAVRE, J. MAY and S. VERHELST. 2012. Recommendations for the new WLTP cycle based on an analysis of vehicle emission measurements on NEDC and CADC. *Energy Policy*, **49**, pp.234-242.
- DFT. 2016. *Vehicle Emissions Testing Programme: Moving Britain Ahead* [online]. [Accessed 22 July 2020]. Available from: https://assets.publishing.service.gov.uk/government/uploads/system/uploads/attachment_data/file/548148/vehicle-emissions-testing-programme-web.pdf.
- DFT. 2020. *Road Traffic Estimates: Great Britain 2019* [online]. [Accessed 12 April 2021]. Available from: <https://www.gov.uk/government/statistics/road-traffic-estimates-in-great-britain-2019>.

- GAO, J., H. CHEN, Y. LI, J. CHEN, Y. ZHANG, K. DAVE and Y. HUANG. 2019. Fuel consumption and exhaust emissions of diesel vehicles in worldwide harmonized light vehicles test cycles and their sensitivities to eco-driving factors. *Energy Conversion and Management*, **196**, pp.605-613.
- GRANGE, S. K., N. J. FARREN, A. R. VAUGHAN, R. A. ROSE and D. C. CARSLAW. 2019. Strong Temperature Dependence for Light-Duty Diesel Vehicle NO_x Emissions. *Environmental Science & Technology*, **53**(11), pp.6587-6596.
- GRUENING, C., P. BONNEL, M. CLAIROTTE, B. GIECHASKIEL, V. VALVERDE, A. ZARDINI and M. CARRIERO. 2019. *Potential of Remote Sensing Devices (RSDs) to screen vehicle emissions* [online]. [Accessed 11 June 2021]. Available from: <https://trimis.ec.europa.eu/content/potential-remote-sensing-devices-screen-vehicle-emissions>.
- GUMBEL, E. J. 1935. Les valeurs extrêmes des distributions statistiques. *Ann. Inst. Henri Poincaré*, **5**(2), pp.115-158.
- HBEFA. 2019. *HBEFA - Handbook Emission Factors for Road Transport (Version 4.1)* [online]. [Accessed 5 August 2020]. Available from: https://www.hbefa.net/e/documents/HBEFA41_Report_TUG_09092019.pdf.
- HUANG, Y., B. ORGAN, J. L. ZHOU, N. C. SURAWSKI, G. HONG, E. F. C. CHAN and Y. S. YAM. 2018. Remote sensing of on-road vehicle emissions: Mechanism, applications and a case study from Hong Kong. *Atmospheric Environment*, **182**, pp.58-74.
- HUANG, Y., B. ORGAN, J. L. ZHOU, N. C. SURAWSKI, Y.-S. YAM and E. F. C. CHAN. 2019. Characterisation of diesel vehicle emissions and determination of remote sensing cutpoints for diesel high-emitters. *Environmental Pollution*, **252**, pp.31-38.
- ICCT. 2018. *Determination of real-world emissions from passenger vehicles using remote sensing data* [online]. [Accessed 7 December 2018]. Available from: <https://www.theicct.org/publications/real-world-emissions-using-remote-sensing-data>.
- ICCT. 2019a. *A comparison of light-duty vehicle NO_x emissions measured by remote sensing in Zurich and Europe* [online]. [Accessed 22 July 2020]. Available from: https://theicct.org/sites/default/files/publications/ICCT_LDV_NOx_emissions_Zurich_20190628_1.pdf.
- ICCT. 2019b. *European vehicle market statistics* [online]. [Accessed 5 August 2020]. Available from: https://theicct.org/sites/default/files/publications/European_vehicle_market_statistics_20192020_20191216.pdf.
- JIMÉNEZ-PALACIOS, J. L. 1999. *Understanding and quantifying motor vehicle emissions with vehicle specific power and TILDAS remote sensing*. thesis, Massachusetts Institute of Technology.
- JOHNSON, T. V. 2009. Diesel emission control in review. *SAE international journal of fuels and lubricants*, **1**(1), pp.68-81.
- LAU, C. F., A. RAKOWSKA, T. TOWNSEND, P. BRIMBLECOMBE, T. L. CHAN, Y. S. YAM, G. MOČNIK and Z. NING. 2015. Evaluation of diesel fleet emissions and control policies from plume chasing measurements of on-road vehicles. *Atmospheric Environment*, **122**, pp.171-182.

- LIN, M., H. C. LUCAS JR and G. SHMUELI. 2013. Research commentary—too big to fail: large samples and the p-value problem. *Information Systems Research*, **24**(4), pp.906-917.
- LOPES, R. H., I. REID and P. R. HOBSON. 2007. The two-dimensional Kolmogorov-Smirnov test. In: *XI International Workshop on Advanced Computing and Analysis Techniques in Physics Research*, April 23-27, 2007, Amsterdam, the Netherlands. Proceedings of Science.
- LOUCKS, P. and E. BEEK. 2017. *Water Resource Systems Planning and Management*.
- LUJÁN, J. M., V. BERMÚDEZ, V. DOLZ and J. MONSALVE-SERRANO. 2018. An assessment of the real-world driving gaseous emissions from a Euro 6 light-duty diesel vehicle using a portable emissions measurement system (PEMS). *Atmospheric Environment*, **174**, pp.112-121.
- MANZIE, C. 2010. CHAPTER THREE - Relative Fuel Economy Potential of Intelligent, Hybrid and Intelligent-Hybrid Passenger Vehicles. In: G. PISTOIA, ed. *Electric and Hybrid Vehicles*. Amsterdam: Elsevier, pp.61-90.
- MASSEY JR, F. J. 1951. The Kolmogorov-Smirnov test for goodness of fit. *Journal of the American statistical Association*, **46**(253), pp.68-78.
- MCCLINTOCK, P. M. 2011. *The Colorado Remote Sensing Program January–December 2010* [online]. [Accessed 11 June 2021]. Available from: <https://downloads.regulations.gov/EPA-R08-OAR-2016-0016-0013/content.pdf>.
- MOODY, A. and J. E. TATE. 2017. In Service CO₂ and NO_x Emissions of Euro 6/VI Cars, Light- and Heavy- dutygoods Vehicles in Real London driving: Taking the Road into the Laboratory. *Journal of Earth Sciences and Geotechnical Engineering*, **7**(1), pp.51-62.
- NAEI. 2021. *UK emissions data selector* [online]. [Accessed 5 July 2021]. Available from: <https://naei.beis.gov.uk/data/data-selector>.
- NTZIACHRISTOS, L., G. PAPADIMITRIOU, N. LIGTERINK and S. HAUSBERGER. 2016. Implications of diesel emissions control failures to emission factors and road transport NO_x evolution. *Atmospheric Environment*, **141**, pp.542-551.
- O'DRISCOLL, R., H. M. APSIMON, T. OXLEY, N. MOLDEN, M. E. J. STETTLER and A. THIYAGARAJAH. 2016. A Portable Emissions Measurement System (PEMS) study of NO_x and primary NO₂ emissions from Euro 6 diesel passenger cars and comparison with COPERT emission factors. *Atmospheric Environment*, **145**, pp.81-91.
- O'DRISCOLL, R., M. E. J. STETTLER, N. MOLDEN, T. OXLEY and H. M. APSIMON. 2018. Real world CO₂ and NO_x emissions from 149 Euro 5 and 6 diesel, gasoline and hybrid passenger cars. *Science of The Total Environment*, **621**, pp.282-290.
- OUARDA, T. B. M. J., C. CHARRON, J. Y. SHIN, P. R. MARPU, A. H. AL-MANDOOS, M. H. AL-TAMIMI, H. GHEDIRA and T. N. AL HOSARY. 2015. Probability distributions of wind speed in the UAE. *Energy Conversion and Management*, **93**, pp.414-434.
- PASTORELLO, C. and G. MELIOS. 2016. *Explaining road transport emissions: a non-technical guide* [online]. European Environment Agency. [Accessed 16 October 2018]. Available from: <https://www.eea.europa.eu/publications/explaining-road-transport-emissions>.

- PAYRI, F., J. J. LOPEZ, B. PLA and D. G. BUSTAMANTE. 2014. *Assessing the limits of downsizing in diesel engines* [online]. SAE Technical Paper. [Accessed 20 May 2021]. Available from: <https://doi.org/10.4271/2014-32-0128>.
- PÖHLER, D., T. ENGEL, U. ROTH, M. HORBANSKI, J. LAMPEL, T. ADLER and U. PLATT. 2019. Real Driving NOx Emissions and Emission Manipulations of Trucks observed with Plume Chasing. *In: Geophysical Research Abstracts*.
- PUJADAS, M., A. DOMÍNGUEZ-SÁEZ and J. DE LA FUENTE. 2017. Real-driving emissions of circulating Spanish car fleet in 2015 using RSD Technology. *Science of The Total Environment*, **576**, pp.193-209.
- ROPKINS, K., T. H. DEFRIES, F. POPE, D. C. GREEN, J. KEMPER, S. KISHAN, G. W. FULLER, H. LI, J. SIDEBOTTOM, L. R. CRILLEY, L. KRAMER, W. J. BLOSS and J. STEWART HAGER. 2017. Evaluation of EDAR vehicle emissions remote sensing technology. *Science of The Total Environment*, **609**, pp.1464-1474.
- RUSHTON, C. E., J. E. TATE and S. P. SHEPHERD. 2021. A novel method for comparing passenger car fleets and identifying high-chance gross emitting vehicles using kerbside remote sensing data. *Science of The Total Environment*, **750**, p142088.
- RUSHTON, C. E., J. E. TATE, S. P. SHEPHERD and D. C. CARSLAW. 2018. Interinstrument comparison of remote-sensing devices and a new method for calculating on-road nitrogen oxides emissions and validation of vehicle-specific power. *Journal of the Air & Waste Management Association*, **68**(2), pp.111-122.
- SHERIF, M., M. ALMULLA, A. SHETTY and R. K. CHOWDHURY. 2014. Analysis of rainfall, PMP and drought in the United Arab Emirates. *International journal of climatology*, **34**(4), pp.1318-1328.
- SJÖDIN, Å., J. BORKEN-KLEEFELD, D. CARSLAW, J. TATE, G.-M. ALT, J. DE LA FUENTE, Y. BERNARD, U. TIETGE, P. MCCLINTOCK and R. GENTALA. 2018. *Real-driving emissions from diesel passenger cars measured by remote sensing and as compared with PEMS and chassis dynamometer measurements-CONOX Task 2 report* [online]. Swiss Federal Office for the Environment (FOEN). [Accessed 14 April 2021]. Available from: <https://www.ivl.se/download/18.34244ba71728fcb3f3fa5a/1591705759623/C294.pdf>.
- SJÖDIN, Å., M. JERKSJÖ, H. FALLGREN, H. SALBERG, R. PARSMO, C. HULT, M.-R. YAHYA, T. WISELL and J. LINDÉN. 2017. *On-Road Emission Performance of Late Model Diesel and Gasoline Vehicles as Measured by Remote Sensing* [online]. IVL Swedish Environmental Research Institute [Accessed 14 April 2021]. Available from: <https://www.ivl.se/download/18.449b1e1115c7dca013adae8/1499086049685/B2281.pdf>.
- SMIT, R., S. BAINBRIDGE, D. KENNEDY and P. KINGSTON. 2021. A decade of measuring on-road vehicle emissions with remote sensing in Australia. *Atmospheric Environment*, **252**, p118317.
- TRIAANTAFYLLOPOULOS, G., A. DIMARATOS, L. NTZIACHRISTOS, Y. BERNARD, J. DORNOFF and Z. SAMARAS. 2019. A study on the CO2 and NOx emissions performance of Euro 6 diesel vehicles under various chassis dynamometer and on-road conditions including latest regulatory provisions. *Science of The Total Environment*, **666**, pp.337-346.

- WANG, C., B. ZENG and J. SHAO. 2011. Application of bootstrap method in Kolmogorov-Smirnov test. *In: 2011 International Conference on Quality, Reliability, Risk, Maintenance, and Safety Engineering*, 17-19 June 2011, pp.287-291.
- WANG, X., D. WESTERDAHL, Y. WU, X. PAN and K. M. ZHANG. 2011. On-road emission factor distributions of individual diesel vehicles in and around Beijing, China. *Atmospheric Environment*, **45**(2), pp.503-513.
- WEISS, M., P. BONNEL, R. HUMMEL, U. MANFREDI, R. COLOMBO, G. LANAPPE, P. LE LIJOUR and M. SCULATI. 2011. Analyzing on-road emissions of light-duty vehicles with Portable Emission Measurement Systems (PEMS). *JRC Scientific and Technical Reports, EUR*, **24697**.
- YANG, Z., J. E. TATE, E. MORGANTI and S. P. SHEPHERD. 2021. Real-world CO₂ and NO_x emissions from refrigerated vans. *Science of The Total Environment*, **763**, p142974.